Reduction of Water/Oil Interfacial Tension by Model Asphaltenes: the Governing Role of Surface Concentration

Cuiying Jian[†,‡,⊥], *Mohammad Reza Poopari*[‡,⊥], *Qingxia Liu*[‡], *Nestor Zerpa*[§]

Hongbo Zeng[‡,*], *and Tian Tang*[†,*]

[†] Department of Mechanical Engineering and

[‡] Department of Chemical and Material Engineering,

University of Alberta, Edmonton, and

[§]Nexen Energy ULC, A CNOOC Limited Company, Calgary

AB, Canada

[*]Corresponding author;

Phone: +1-780-492-1044. Fax: +1-780-492-2881. E-mail: hongbo.zeng@ualberta.ca (H.Z.)

Phone: +1-780-492-5467. Fax: +1-780-492-2200. E-mail: tian.tang@ualberta.ca (T.T.)

[⊥]These authors contributed equally to this work.

Abstract:

In this work, pendant drop techniques and molecular dynamics (MD) simulations were employed to investigate the effect of asphaltene concentrations on the interfacial tension (IFT) of oil/water interface. Here, oil and asphaltene were represented by, respectively, common organic solvents and Violanthrone-79, and two types of concentration, i.e. bulk concentration and surface concentration, were examined. Correlations between the IFTs from experiments and MD simulations revealed that surface concentration, rather than the commonly used bulk concentration, determines the reduction of oil/water IFTs. Through analyzing the hydrogen bonding, the underlying mechanism for the IFT reduction was proposed. Our discussions here not only enable the direct comparison between experiments and MD simulations on the IFTs but also help with future interfacial studies using combined experimental and simulation approaches. The methodologies used in this work can be extended to many other oil/water interfaces in the presence of interfacially active compounds.

1. Introduction

During petroleum processing, the undesired water-in-oil emulsions are usually stabilized by asphaltenes, and being prevented from coalescences.[1, 2] These emulsified droplets possess serious effects, such as fouling on and corroding the pipelines and plant equipment, intriguing safety issues and generating additional costs for the water and oil separation.[3-5] Significant efforts have been devoted to investigating the stabilization effect of asphaltenes and emulsion drops as well as the underlying mechanisms.

One experimentally measurable quantity that can help to understand the emulsion stability is the interfacial tension (IFT) of oil/water interface.[6, 7] With the presence of asphaltenes, the IFT of oil/water interface decreases, which indicates the adsorption of asphaltenes onto the interface and thus hindering the coalescences of water droplets.[6, 8] In addition, IFT can also be correlated to other important quantities, such as interfacial excess through the Gibbs adsorption isotherm[9-11] and critical micelle concentrations[9]. Therefore, IFT parameters have been widely measured in experiments with the presence of asphaltene compounds under different conditions.[12, 13]

Despite the great importance of IFT, very few computational works are available in literature for oil/water interface in presence of asphaltene molecules. For instance, while molecular dynamics (MD) simulations have been widely adopted to investigate the bulk aggregation behaviors as well as interfacial structures of asphaltene compounds,[14-27] little MD investigation has been performed to probe the effect of asphaltenes on the IFTs of oil/water interface. Only very recently, Mikami et al.[28] performed a series of MD simulations to investigate

the effect of their representative asphaltene compounds on the IFT of heptane/water interface. Similar to experimental findings[8, 28-30], Mikami et al.[28] reported that increasing the concentration of asphaltene molecules decreased the IFT. However, large discrepancy exists on the concentrations used in simulations and experiments. Specifically, in the simulation work of Mikami et al.[28], a dramatic reductions on the IFT were only observed when a complete thin film of asphaltene molecules was formed between the heptane and water phases. That is, an extremely high bulk concentration (42 wt %, 483 g/L) of asphaltenes in heptane is needed in order to decrease the IFTs of the heptane/water interface. In contrast, experiments reported that IFT can be decreased by asphaltenes at very low bulk concentrations. For instance, for heptol/water interface, IFT reduction was reported by Gao et al.[8] (toluene-heptane volume ratio 4:1) at 0.1 wt % of asphaltenes, and by Fan et al.[30] (toluene-heptane volume ratio 6:4) at 2~5 g/L of asphaltenes. Apparently, even taking into consideration the difference in the type of solvents and solutes, great discrepancies exist between experiments and simulations regarding the concentrations at which an IFT reduction can be observed. Therefore, there is still lack of a clear understanding on the effect of concentration in decreasing the IFT of oil/water interface. The answer to this question will not only help with improving comparison on the IFT between experiments and simulations but also provide important foundations for probing the interfacial properties of asphaltenes using theoretical modeling, and thus further providing atomic information for the emulsion problems encountered in petroleum processing.

In this work, adopting Violanthrone-79 (VO-79), a common surrogate for asphaltenes,[31, 32] we performed a series of experimental and theoretical studies to probe the role of concentrations on reducing the IFTs of oil/water interface. The oil phase is represented using

common organic solvents, e.g. toluene and n-heptane, and two types of concentrations were discussed, namely bulk concentration and surface concentration. Through direct comparison between the results from MD simulations and experimental measurements, the governing factor on the IFT reduction was clarified. The remainder of this article is organized as follows: the experimental setup and simulated systems are introduced in section 2; section 3 presents detailed analysis on the role of bulk concentration and surface concentration in reducing the IFT; and final conclusions are given in section 4.

2. Methods

2.1. Experimental. *Materials.* The model asphaltene compound VO-79 ($C_{50}H_{48}O_4$, structure shown in Figure 1) has one large polyaromatic core and two long aliphatic side chains, similar to the island-type structure proposed for asphaltene molecules in literature.[33] Compared to experimentally measured average weight percentage of oxygen in real asphaltenes, ≤1.50% as reported by Sato et al.[34], the oxygen content in VO-79 is relatively high (9.0%). On the other hand, it is close to that of the asphaltene fractions stabilizing oil/water emulsions, 5.54% as reported by Yang et al.[35] The VO-79 compound was obtained from Alfa Aesar, and the solvents, i.e. distilled water, n-heptane, and toluene, were purchased from Sigma-Aldrich. All reagents were analytical grade and used as received without further modification.

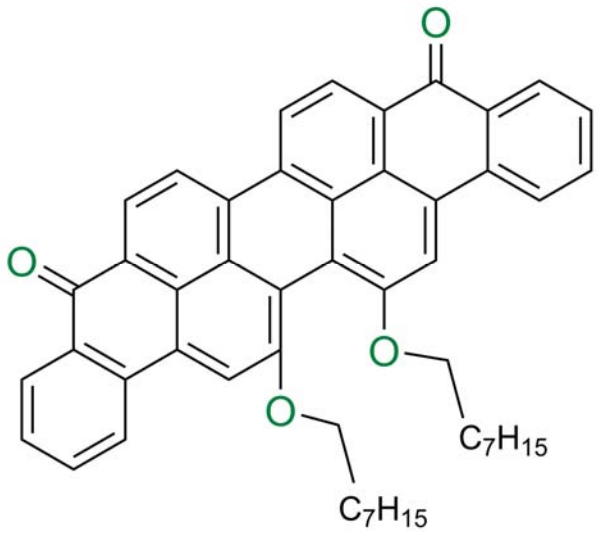

Figure 1. Chemical Structure of VO-79 compound.

Two types of solutions were prepared, one having VO-79 in toluene and the other having VO-79 in heptol. For VO-79 in toluene, three concentrations were employed, 50, 1000, and 5000 ppm; for VO-79 in heptol, the solvent (heptol of n-heptane/toluene mass ratio 1:1, corresponding to volume ratio 56:44) was first obtained by mixing n-heptane and toluene. Then, appropriate amount of VO-79 was added to achieve a concentration of 50 ppm.

IFT Measurements. For the IFT measurements, a two-step process was used. Firstly, pendant droplets of organic solutions were formed in aqueous environments. To achieve so, the VO-79 solutions were loaded into a syringe connected to a U-shape needle. Then the needle was inserted into a quartz cell containing distilled water (dispersion medium), and by moving the plunger downward, a pendant droplet of volume 20-30 μL was formed at the tip of the needle. The so-formed droplet was illuminated by means of a light source and a high speed CCD camera was

used to capture the droplet profile. All experiments were conducted using a rame-hart tensiometer at room temperature and 1 atm pressure, and the droplet profiles were captured every 2 s for a total period of 4000 s.

From the droplet profiles, the IFT was then calculated by applying the following equation[36]:

$$\gamma = [\Delta\rho . g . (R_0)^2] / \beta, (1)$$

where $\Delta\rho$ is the mass density difference between the droplet phase (solution of VO-79 in organic solvent) and the surrounding medium (water), g is the gravity constant, R_0 is the radius of curvature at the droplet apex (approximating the local geometry as part of a sphere), and β is the shape factor. The DROPimage software was used to obtain the size parameters (R_0 and β) for the droplets, and further calculate the IFTs.

2.2. Simulation. *Systems Simulated.* The initial structure of VO-79 molecules was built using Chem3D Ultra 10.0. Organic solvents, toluene and n-heptane, were equilibrated in our previous simulations[20, 21] and directly adopted here; heptol of different n-hepatne/toluene volume ratios (56:44 and 80:20, corresponding to, respectively, 50:50 and 75:25 mass ratios) were developed using the procedures described in our earlier work.[22] A total of 16 simulations were designed to probe the IFT trend with varying solvents as well as concentrations, and their information is summarized in Table 1.

Table 1. Details of the Systems Simulated

Sim. No.	systems	no. of toluene molecules	no. of n-heptane molecules	no. of VO-79 molecules	bulk concn. (ppm)	bulk concn. (g/L)
1	4-H	0	6347	4	4464	2.74
2	4-HT80	1721	5145	4	4212	2.74
3	4-HT56	3814	3664	4	3953	2.74
4	4-T	8900		4	3465	2.74
5	32-H	0	5970	32	36735	21.93
6	32-HT80	1640	4824	32	35321	21.93
7	32-HT56	3631	3439	32	33036	21.93
8	32-T	8416	0	32	28579	21.93
9	90-H	0	5536	90	103674	61.68
10	150-H	0	5528	150	161816	102.80
11	180-H	0	5421	180	191095	123.36
12	540-H	0	3417	540	529271	370.08
13	90-T	7772	0	90	82231	61.68
14	150-T	7797	0	150	129567	102.80
15	180-T	7613	0	180	154649	123.36
16	540-T	4883	0	540	461109	370.08

The first 4 systems in Table 1 involve 4 VO-79 molecules as the solutes. During construction of the initial configuration for each system, a box of dimension 12×12×12 nm^3 was first randomly filled with water molecules (see a schematic illustration in Figure 2a). The box was then expanded in the z-driection to a length of 24 nm, and 4 VO-79 molecules were packed into the empty space with their polyaromatic cores parallel with one another. The rest of the box was filled with n-heptane in system 4-H, heptol of 80% (volume percentage) n-heptane in system 4-HT80, heptol of 56% n-heptane in system 4-HT56, or toluene in system 4-T. While only 4 solute molecules were employed here, the resultant systems had VO-79 mass concentration of ~4000 ppm (0.4 wt %) in organic solvents, close to a bulk concentration of 5000

ppm employed in our experiments. To study the effect of concentration, the number of VO-79 molecules was then increased to 32, corresponding to simulations 5 to 8 in Table 1. These 4 simulations are of bulk concentrations > 28000 ppm (2.8 wt%), which is far above those in our experimental studies as well as those usually employed in other experimental studies[8, 30].

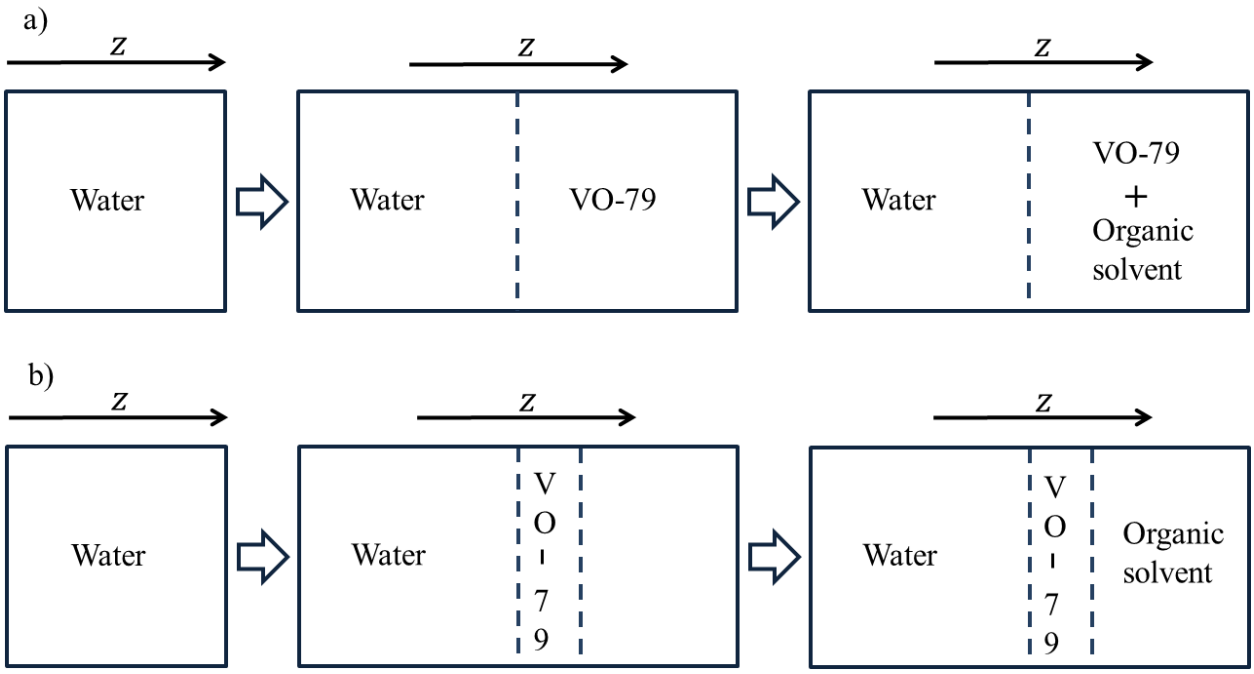

Figure 2. Schematic representations for two ways of constructing the initial configurations: a) simulations 1 to 8 where VO-79 are solvated in the organic solvent; and b) simulations 9-16 where VO-79 are packed on the interface between water and organic solvent.

To probe the role of surface concentration on IFT, 8 additional simulations were designed. The initial configurations for these 8 systems were constructed using the scheme described in Figure 2b. Briefly, we placed, between the water phase and the organic solvent phase, a single layer of VO-79 molecules in simulations 9-11 and 13-15 listed in Table 1. For systems 90-H and

90-T (simulations 9 and 13), the layer contains 90 VO-79 molecules on the interface; the number is increased to 150 in systems 150-H and 150-T, and to 180 in systems 180-H and 180-T. With 180 molecules, the interface is completely covered (100% surface coverage in the initial configuration). We then introduced two additional layers of VO-79 molecules and formed a three-layer interface in systems 540-H and 540-T (simulations 12 and 16 in Table 1). In each of these 8 systems, the VO molecules were initially arranged to have their polyaromatic cores parallel with one another.

Simulation Details. The VO-79 topology was obtained by first submitting its initial coordinates to the GlycoBioChem PRODRG2 server.[37] The partial charges and charge groups in the default topology from PRODRG was then manually adjusted to be compatible with the GROMOS96 force field parameter set 53A6.[38] The validation for this approach of creating topology has been justified in our previous work.[19] For solvent molecules, a simple-point-charge (SPC) model[39] was used for water, which has been extensively tested for interfacial studies[27,28]; the topology for toluene and n-heptane were validated in our earlier work[20, 21] and directly adopted here.

All the simulations were performed using the MD package GROMACS[40-43]. For each system, static energy minimization was first performed to ensure that the maximum force is less than 1000.0 kJ/(mol*nm). Then $NP_{normal}AT$ ensemble simulations were performed for 40 ns for simulations 1-8 in Table 1, and for 10 ns for simulations 9-16. Here, P_{normal} and A represent, respectively, iso-normal pressure perpendicular to the interface (z direction in Figure 1), and iso-

interfacial area. It should be mentioned here the capability of $NP_{normal}AT$ ensemble for predicting IFT in MD has been widely justified in literature[44, 45].

During the full dynamic simulation, Parrinello-Rahman barostat[46] was used to keep the average normal pressure at 1 bar, and a velocity rescaling thermostat,[47] based on correctly producing the probability distribution of kinetic energy under constant temperature, was used to keep the average temperature at 300 K. In all the simulations, periodic boundary conditions, full electrostatics with particle-mesh Ewald method,[48] cutoff distance of 1.4 nm for van der Waals, SETTLE algorithm[49] to constrain all bonds for water molecules, LINCS algorithm[50] to constrain all bonds for solute as well as organic solvent molecules, and a time step of 2 fs were used.

Data Analysis. The IFT of each system is calculated using the following equation[51]:

$$\gamma = \frac{1}{2}(p_z - \frac{p_x+p_y}{2})L_z, \quad (2)$$

where p_x, p_y and p_z are the diagonal components of the pressure tensor, and L_z is the box length in z direction. As a benchmarking study, we first calculated IFTs of the organic solvents with SPC water in absence of the VO-79 molecules and the results are given in Supporting Information (section S1). While experimental value for heptol/water IFT is not available, the comparison between simulation and experimental data on IFT of pure n-heptane and toluene with water showed good agreements. Together with other reported work where IFT was evaluated using Eq. (1), this justifies our approach to evaluate IFT from MD simulations.[45, 51, 52]

In the result section below, appropriate post-processing tools available in GROMACS were used for trajectory analysis and VMD[53] used for visualization. Unless otherwise specified, all analysis was based on the last 5 ns of the simulation for the first 8 system in Table 1 and the last 2 ns for all the other systems in Table 1. Demonstration for the achievement of dynamic equilibrium is available in the Supporting Information, section S2.

3. Results and Discussion

3.1. Correlation of IFT with Bulk Concentrations. The IFTs obtained in our experimental studies were plotted as a function of time in Figure 3. Clearly, the final plateau values of IFTs greatly depend on the solvents and the concentrations of VO-79 employed. For instance, with increasing toluene ratio (Figure 3a), the IFT was decreased from ~38 mN/m to 33 mN/m; for pure toluene solvent, while the reduction on IFT is small from 50ppm to 1000ppm, a dramatic reduction on the IFT was observed when the bulk concentration of VO-79 reached 5000 ppm (Figure 3b). Both observations are consistent with literature works[8, 28-30] reported earlier, and thus justifying our experimental methodology. Moreover, detailed inspection of Figure 3 shows that IFT is decreasing with time, particularly at high bulk concentrations (5000 ppm in Figure 3b). This indicates the continuing migration of VO-79 molecules from bulk solutions to the interface, which introduce further reductions to the IFTs.

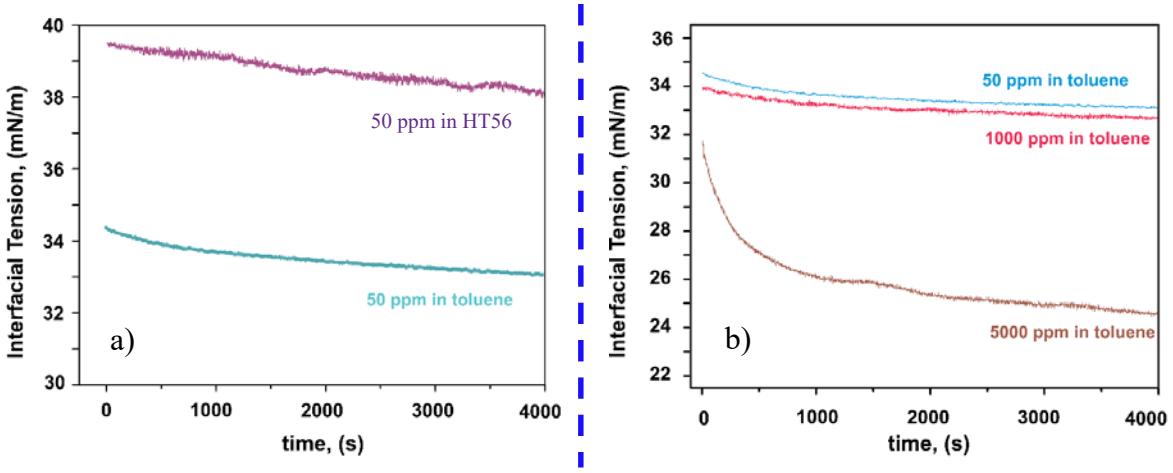

Figure 3. IFT between the organic solution and water as a function of time a) for VO-79 in HT56 (heptol of n-heptane-toluene volume ratio 56:44) and toluene at a bulk concentration of 50 ppm and b) for VO-79 in toluene at three different bulk concentrations: 50, 1000, and 5000 ppm.

Theoretical calculations were first carried out for systems with VO-79 molecules initially dispersed in organic solvents, i.e. systems 1-8 in Table 1. The obtained IFTs are plotted in Figure 4, each solvent being represented by a certain color and lines drawn for a guide of eyes. As the solvent is changed from 100% n-heptane to 100% toluene, the IFTs shows a monotonic decrease, consistent with our experimental observation and the results reported by Hu et al.[29] on asphaltenes at the heptol/brine interface. On the other hand, surprisingly, regardless of the concentration, the calculated IFTs are close to the values in absence of the VO-79 molecules. For instance, in system 32-T with a bulk concentration of 28579 ppm, an IFT value of 35 mN/m was obtained using MD, similar to 35.3 mN/m for pure toluene. Contrarily, at a bulk concentration of 5000 ppm in toluene, the IFT was decreased to a plateau value of 24 mN/m in our experimental study. Furthermore, evident reductions on IFT have also been reported for similar compounds at

very low bulk concentrations in experiments. For instance, compared to the IFT value (36.5 mN/m) for pure toluene/water interface at pH 9[54], Norgard et al.[55] reported that the presence of BisA, a model asphaltene compound for which ketone groups are the only explicit polar groups, decreased the IFT value to 32 mN/m with a bulk BisA concentration of only 50 μM (~44 ppm). Clearly, evident discrepancies exist between simulations and experiments regarding the effect of concentrations. To understand these seemingly discrepancies, below we will take a detailed look at our simulated systems.

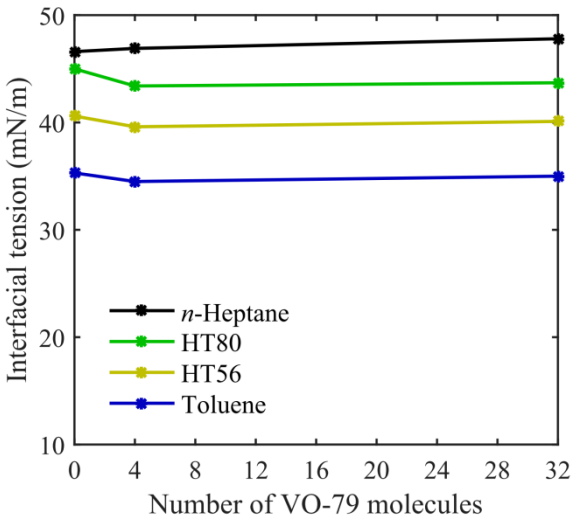

Figure 4. IFT values versus number of VO-79 molecules in each solvent. Lines are drawn for a guide of eyes.

Compared to toluene, n-heptane is a "poor" solvent for the VO-79 molecules studied here. It's thus expected VO-79 molecules will prefer to migrate to the interface in n-heptane. Figure 5 shows the final configuration formed in systems 4-H and 32-H. As it can be seen, all VO-79 molecules indeed migrated to the interface, and the adsorbed molecules prefer an aggregated

state with their polyaromatic cores being perpendicular to the interface. This is consistent with the experimental study by Andrews et al.[56], where the same orientation was found for similar molecules (Violanthrone-78, VO-78) on the hydrophilic CaF_2 surface. It's worth pointing out that the specific configuration of VO-79 obtained here can be dependent on the molecular structure employed and might differ from that of real asphaltenes extracted from crude oils.[57] For example, Andrews et al.[56] pointed out that unlike VO-78, certain real asphaltenes tend to possess orientations with their polyaromatic cores parallel to the interface, and such difference can be attributed to the oxygen functionality present in VO-78.

On the other hand, while all VO-79 molecules indeed migrated to the interface as shown in Figure 5, majority of the interface is still dominant by the water-n-heptane contact, which can be further verified by calculating the distribution of different types of molecules with respect to the interface as shown in the Supporting Information (section S3). This is why no dramatic changes were observed in the IFT with increasing the bulk concentration of VO-79 in our simulations. Interestingly, through a series of IFT measurements, Yeung *et al.*[52, 58] also reported that the IFT of a given interface is not solely determined by the bulk concentration of solutes. Specifically, different experiments were designed to create heptol/water interfaces with different configurations: a centimeter-sized heptol layer on top of water, a millimeter-sized heptol droplet in a water bath or a macroemulsion having a large number of micrometer-sized water droplets in heptol. In all cases, there were surfactants in the heptol solution and the bulk concentration of the surfactant was kept the same in all experiments. The different experiments, however, rendered different IFT values. From the results, it was proposed that IFT is a function of the ratio between the volume of the liquid phase (volumes of heptol and water in their experiments are of similar

scales) and the interfacial area. That is, at the same bulk concentrations, the concentration of surfactants at interface can be different. For our current work, the length scale used in the simulations (~nm) is seven orders of magnitude smaller than that (~cm) in our experiments. Therefore, it is possible that while much higher bulk concentrations were employed in MD simulations compared to those in experiments, the surface concentration of solute molecules at the interface in the simulations may still be much lower than the corresponding ones in the experiments. To verify our hypothesis, in the following section, we first analyzed the surface concentration of VO-79 molecules in details.

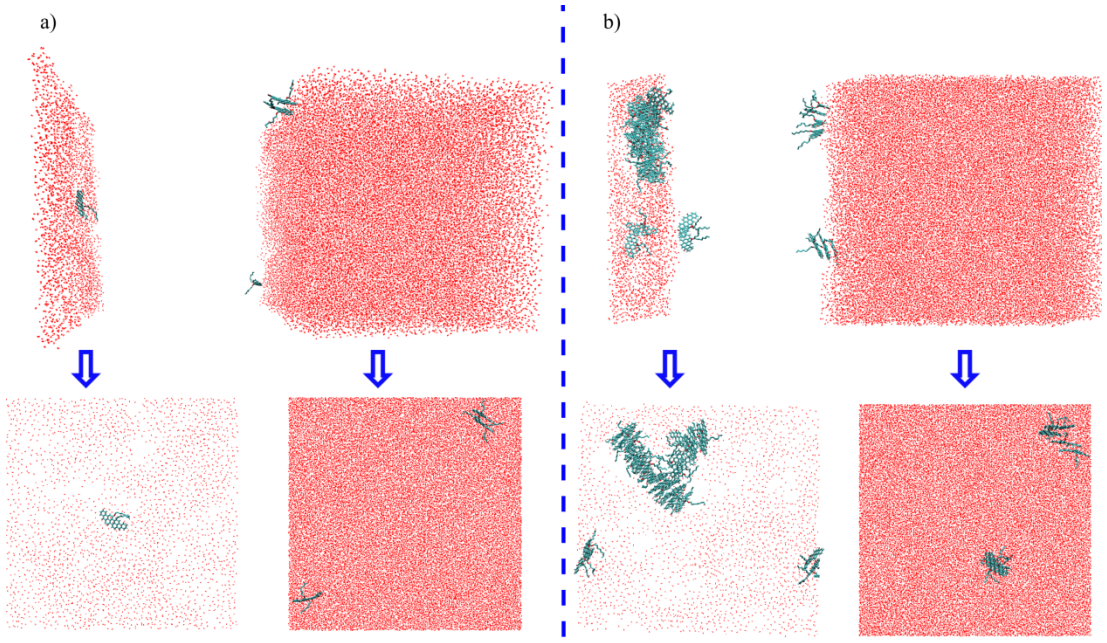

Figure 5. Final configurations formed in systems: a) 4-H, top pane, side view; bottom pane, axis view; and b) 32-H, top pane, side view, bottom pane, axis view. Water molecules are shown in red and VO-79 molecules in cyan. n-Heptane molecules are not shown for clarity.

3.2. Correlation of IFT with Surface Concentrations. The surface excess in our experiments is calculated using Gibbs adsorption isotherm[59]:

$$\Gamma = -\frac{1}{RT}\frac{d\gamma}{d\ln c}, \quad (3)$$

where Γ and c are the surface excess (mol/m^2) and concentration (mol/L) of the solute (the initial bulk concentrations of VO molecules in toluene shown in our experimental studies), R is the universal gas constant (J/(K×mol)), T is temperature (K) and γ is the IFT (N/m). To calculate Γ, the IFT data at 1000 ppm and 5000 ppm were employed. The reason for omitting the data point at 50 ppm is that only when c is sufficiently high can the interface be considered saturated with solute molecules, resulting in nearly constant surface excess.[59] For instance, in the case of surfactant being the solutes, c needs to be below but close to the critical micelle concentration.[59] Therefore, from our experimental results: $\Gamma = -\frac{1}{8.314\times300}\frac{(24.8-33.6)\times10^{-3}}{(\ln(6.08\times10^{-3})-\ln(1.22\times10^{-3}))}\frac{\text{mol}}{\text{m}^2} = 2.20\times10^{-6}$ mol/m^2, and by taking the Avogadro constant into consideration, the corresponding surface concentration is 1.32 molecule/nm^2.

The surface concentration of VO-79 molecules in the MD simulations is estimated by dividing the number of VO-79 molecules on the interface over the interfacial area. For instance, in system 4-H, the interfacial area is $12\times12 = 144$ nm^2 and all of the 4 VO-79 molecules migrated to the interface, resulting in a surface concentration $4/144 = 0.03$ molecule / nm^2. This represents the highest surface concentration among simulations 1 to 4, since not all VO-79 molecules migrate to the interface in presence of toluene solvent. On the other hand, in experiments, at a bulk concentration of 5000 ppm (similar to that in the systems having 4 VO

molecules) in toluene, the surface concentration is much higher (1.32 molecule/nm^2) as shown in the preceding paragraph. That is, at similar bulk concentration, surface concentrations in the simulations can be very different from those in experiments, which can be the reason why there is a discrepancy between the reduced IFT in experiments and the constant IFT in simulations.

To further probe the effect of surface concentration on the IFT, we introduced more VO-79 molecules to the simulation systems (simulations 9-16 in Table 1). As it can be seen from Figure 3, migration of the solute molecules onto the interface can take as long as 4000 s, which is impossible to observe within the simulation time (hundreds of ns) affordable by current computational techniques. Therefore for simulations 9-16 in Table 1, VO-79 molecules were directly placed at the interface in the initial configuration (Figure 2b). Figure 6 summarizes the IFT calculated for the systems simulated in n-heptane and toluene. Clearly, the IFT shows a monotonic decrease as the number of VO-79 molecules is increased from 90 to 540, consistent with our experimental study and other experimental works[8, 28-30] on the effect of concentration in literature. Furthermore, the most drastic decrease is observed when the number of VO-79 molecules reaches 180. While this number corresponds to extremely high bulk concentrations (191095 ppm and 154649 ppm, respectively, in systems 180-H and 180-T), the corresponding surface concentration is $18/144 = 1.25$ molecule / nm^2, close to the saturated surface concentration (1.32 molecule / nm^2) in our experimental studies. This suggests that the IFTs are governed by the surface concentration of interfacially active molecules rather than their bulk concentration. It is of great importance to point out here that similar conclusions have also been validated in the field of surfactants. For instance, in the work of Hu et al.[60], the IFT values obtained from MD has been compared to those in the experimental work of Pradines et al.[61] for

surfactant sodium dodecyl sulfate. The results from these two works are in good agreement at similar surface concentrations, while these surface concentrations correspond to distinct bulk concentrations. For example, at surface concentration ~1 molecule/nm^2, the bulk concentrations are, respectively, 0.36 mol/L in the simulation work[60] and 0.001 mol/L in the experimental work [61], which differ by two orders of magnitude.

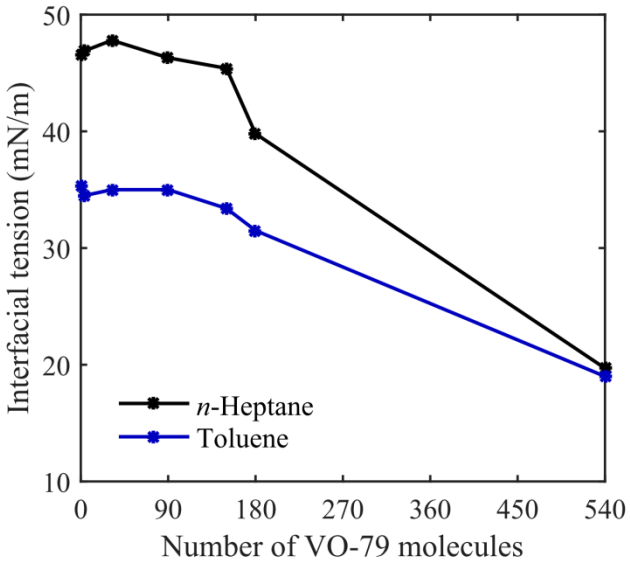

Figure 6. IFT obtained for systems simulated in n-heptane and toluene.

In literature, there has been a great barrier for comparisons between experiments and simulations on the effect of concentrations. The reason is that to accommodate the bulk concentrations in experiments, very few molecules can be put into a relatively small simulation box. For instance, as shown in section 2, when only 4 VO-79 molecules are placed in a cubic box of dimensions 12×12×12 nm^3, the bulk concentration is already ~3000 ppm. However, as revealed here, it is the surface concentration, instead of bulk concentration, that governs the reduction of IFT. This provides justifications for MD simulations to employ high bulk

concentrations in order to achieve the same surface concentration as that in experiments. It is of great importance to emphasize that not only are our results applicable to model compounds employed to mimic asphaletenes, they also have direct implications for real asphaltenes. For instance, Banerjee and co-workers[57, 62, 63] investigated the effect of real asphaltenes on the IFT of water/model oil (mixtures of aliphatic base oil and toluene) interface under a variety of experimental conditions (including different bulk concentrations of asphaltenes). A universal relation was derived between the IFT and surface coverage (similar to surface excess calculated in our work) of asphaltenes, where the IFT monotonically decreases with increasing surface coverage, consistent with our findings here. However in their work, differences between bulk and surface concentrations in affecting the IFT are not explicitly discussed. Therefore the results reported here help to draw a comprehensive picture on the effect of asphaltene concentration.

3.3. Mechanisms of the IFT Reductions. In Figure 6, a larger decrease in IFT is observed for the systems in n-heptane compared to those in toluene. For instance, while in absence of VO-79 molecules, the n-heptane-water interface is of a much higher IFT than that of toluene-water interface, as VO-79 molecules are added and accumulate on the interface, the IFTs converge to 20 mN/m in both n-heptane and toluene. As oxygen functionality is presented in the molecular structure of VO-79, it is expected that hydrogen bonds can be formed between VO-79 and water molecules. Therefore we calculated the number of hydrogen bonds formed between VO-79 and water molecules at the equilibrium stage in simulations 9-16 and the results were plotted in Figure 7. Here, a geometric criterion of Donor − Acceptor distance $r_{DA} \leq 0.35$ nm and Acceptor – Donor – Hydrogen angle $\theta_{ADH} \leq 30^{\circ}$ was used.

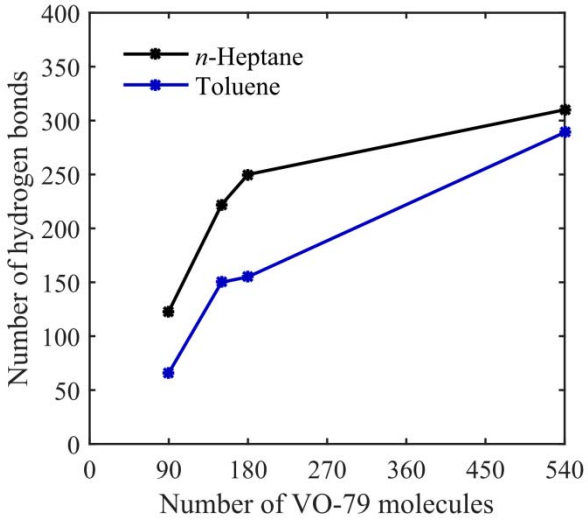

Figure 7. Number of hydrogen bonds formed in simulations 9-16 in Table 1.

From Figure 7, generally, larger numbers of hydrogen bonds are formed in n-heptane compared to toluene, consistent with the larger reductions on IFTs for the systems in n-heptane as shown in Figure 6. The less hydrogen bonds formed in toluene indicates the slight migration of VO-79 molecules from the interface to the bulk toluene phase, which resulted from the fact that toluene is a "good" solvent for these polyaromatic molecules[20, 21] (for more discussion on solvent effects, see Supporting Information, section S4). Detailed examination of Figure 7 also reveals that in both n–heptane and toluene, the number of hydrogen bonds can be correlated to the number of VO-79 molecules, and has the following order: 540-H (T) > 180-H(T) and 150-H(T) > 90-H(T). That is, the number of hydrogen bonds shares the opposite trend to that of IFT. Furthermore at sufficient high concentration of VO-79 molecules, i.e. 540 VO-79 molecules, where the organic solvent is being separated from contacting with water phase, similar numbers of hydrogen bonds were formed in n–heptane and toluene, corresponding to the similar

converged IFT values observed in Figure 6. Therefore, as explicit hydrogen bonding cannot be formed between organic solvents (toluene or n-heptane) and water, it can be concluded that the hydrogen bonding formation between VO-79 (interfacially active compound) and water is at least one of the mechanisms that reduces the IFT in the presence of VO-79 molecules. Moreover, hydrogen bonding is originated from electrostatic forces, and hence other types of electrostatic forces which can be enhanced by the presence of VO-79 molecules, such as induced dipole-induced dipole interaction between VO-79 and water molecules, may also play an important role in reducing the IFT.

4. Conclusions

In this work, we investigated the effects of model asphaltene concentration on the water/oil IFT. Two types of concentration were considered here, namely, bulk concentration and surface concentration. The experimental surface concentration of the model asphaltenes was calculated using the Gibbs adsorption isotherm. Through detailed analysis on the IFT values obtained from MD simulations and experimental pendant drop techniques, it was revealed that reductions of the water/oil IFT are governed by the surface concentration of model asphaltenes, while the corresponding bulk concentration can be dramatically different. That is, correlations of the IFT should be made based on surface concentration of the solutes. Furthermore, with increasing the surface concentration of model asphaltenes, number of hydrogen bonds formed between model asphaltene and water molecules demonstrated an opposite pattern compared to that of the IFT, which suggests that hydrogen bonding formation between VO-79 and water molecules is one of the driving forces that reduces the oil/water IFT. The results reported here provide justifications

for direct comparison between MD simulations and experiments on the interfacial behaviors of asphaltenes, and the methodologies can be extended to many other oil/water interfaces in the presence of interfacailly active compounds.

Acknowledgement

We acknowledge the computing resources and technical support from Western Canada Research Grid (WestGrid). Financial support from the Natural Science and Engineering Research Council (NSERC) of Canada and Canadian Centre for Clean Coal/Carbon and Mineral Processing Technologies (C^5MPT) is gratefully acknowledged.

Supporting Information

IFTs of the organic solvents with SPC water in absence of VO-79 molecules, demonstration for the achievement of dynamic equilibrium, distribution of different types of molecules with respect to the interface, and solvent effects for solvating VO-79 molecules.

References

(1) McLean, J. D.; Kilpatrick, P. K. Effects of Asphaltene Solvency on Stability of Water-in-Crude-Oil Emulsions. *J. Colloid Interface Sci.* **1997**, *189*, 242-253.

(2) Nenningsland, A. L.; Gao, B.; Simon, S.; Sjöblom, J. Comparative Study of Stabilizing Agents for Water-in-Oil Emulsions. *Energy Fuels* **2011**, *25*, 5746-5754.

(3) Mouraille, O.; Skodvin, T.; Sjöblom, J.; Peytavy, J. Stability of Water-in-Crude Oil Emulsions: Role Played by the State of Solvation of Asphaltenes and by Waxes. *J. Dispersion Sci. Technol.* **1998**, *19*, 339-367.

(4) Spiecker, P. M.; Gawrys, K. L.; Trail, C. B.; Kilpatrick, P. K. Effects of Petroleum Resins on Asphaltene Aggregation and Water-in-Oil Emulsion Formation. *Colloids Surf. Physicochem. Eng. Aspects* **2003**, *220*, 9-27.

(5) Kilpatrick, P. K. Water-in-Crude Oil Emulsion Stabilization: Review and Unanswered Questions. *Energy Fuels* **2012**, *26*, 4017-4026.

(6) Poteau, S.; Argillier, J.; Langevin, D.; Pincet, F.; Perez, E. Influence of pH on Stability and Dynamic Properties of Asphaltenes and Other Amphiphilic Molecules at the Oil-Water Interface. *Energy Fuels* **2005**, *19*, 1337-1341.

(7) Yan, Z.; Elliott, J. A.; Masliyah, J. H. Roles of various Bitumen Components in the Stability of Water-in-Diluted-Bitumen Emulsions. *J. Colloid Interface Sci.* **1999**, *220*, 329-337.

(8) Gao, S.; Moran, K.; Xu, Z.; Masliyah, J. Role of Naphthenic Acids in Stabilizing Water-in-Diluted Model Oil Emulsions. *The Journal of Physical Chemistry B* **2010**, *114*, 7710-7718.

(9) Rogel, E.; Leon, O.; Torres, G.; Espidel, J. Aggregation of Asphaltenes in Organic Solvents using Surface Tension Measurements. *Fuel* **2000**, *79*, 1389-1394.

(10) Bouriat, P.; El Kerri, N.; Graciaa, A.; Lachaise, J. Properties of a Two-Dimensional Asphaltene Network at the Water-Cyclohexane Interface Deduced from Dynamic Tensiometry. *Langmuir* **2004**, *20*, 7459-7464.

(11) Horváth-Szabó, G.; Masliyah, J. H.; Elliott, J. A.; Yarranton, H. W.; Czarnecki, J. Adsorption Isotherms of Associating Asphaltenes at oil/water Interfaces Based on the Dependence of Interfacial Tension on Solvent Activity. *J. Colloid Interface Sci.* **2005**, *283*, 5-17.

(12) Acevedo, S.; Escobar, G.; Gutiérrez, L.; Rivas, H. Isolation and Characterization of Natural Surfactants from Extra Heavy Crude Oils, Asphaltenes and Maltenes. Interpretation of their Interfacial Tension-pH Behaviour in Terms of Ion Pair Formation. *Fuel* **1992**, *71*, 619-623.

(13) Fossen, M.; Kallevik, H.; Knudsen, K. D.; Sjöblom, J. Asphaltenes Precipitated by a Two-Step Precipitation Procedure. 1. Interfacial Tension and Solvent Properties. *Energy Fuels* **2007**, *21*, 1030-1037.

(14) Headen, T. F.; Boek, E. S.; Skipper, N. T. Evidence for Asphaltene Nanoaggregation in Toluene and Heptane from Molecular Dynamics Simulations†. *Energy Fuels* **2009**, *23*, 1220-1229.

(15) Teklebrhan, R. B.; Ge, L.; Bhattacharjee, S.; Xu, Z.; Sjöblom, J. Probing Structure–Nanoaggregation Relations of Polyaromatic Surfactants: A Molecular Dynamics Simulation and Dynamic Light Scattering Study. *The Journal of Physical Chemistry B* **2012**, *116*, 5907-5918.

(16) Sedghi, M.; Goual, L.; Welch, W.; Kubelka, J. Effect of Asphaltene Structure on Association and Aggregation using Molecular Dynamics. *The Journal of Physical Chemistry B* **2013**, *117*, 5765-5776.

(17) Frigerio, F.; Molinari, D. A Multiscale Approach to the Simulation of Asphaltenes. *Computational and Theoretical Chemistry* **2011**, *975*, 76-82.

(18) Kuznicki, T.; Masliyah, J. H.; Bhattacharjee, S. Molecular Dynamics Study of Model Molecules Resembling Asphaltene-Like Structures in Aqueous Organic Solvent Systems. *Energy Fuels* **2008**, *22*, 2379-2389.

(19) Jian, C.; Tang, T.; Bhattacharjee, S. Probing the Effect of Side Chain Length on the Aggregation of a Model Asphaltene using Molecular Dynamics Simulations. *Energy Fuels* , .

(20) Jian, C.; Tang, T.; Bhattacharjee, S. Molecular Dynamics Investigation on the Aggregation of Violanthrone78-Based Model Asphaltenes in Toluene. *Energy Fuels* **2014**, .

(21) Jian, C.; Tang, T. One-Dimensional Self-Assembly of Poly-Aromatic Compounds Revealed by Molecular Dynamics Simulations. *The Journal of Physical Chemistry B* **2014**, .

(22) Jian, C.; Tang, T. Molecular Dynamics Simulations Reveal Inhomogeneity-Enhanced Stacking of Violanthrone-78-Based Polyaromatic Compounds in n-Heptane–Toluene Mixtures. *The Journal of Physical Chemistry B* **2015**, *119*, 8660-8668.

(23) Gao, F.; Xu, Z.; Liu, G.; Yuan, S. Molecular Dynamics Simulation: The Behavior of Asphaltene in Crude Oil and at the Oil/Water Interface. *Energy Fuels* **2014**, *28*, 7368-7376.

(24) Teklebrhan, R. B.; Ge, L.; Bhattacharjee, S.; Xu, Z.; Sjöblom, J. Initial Partition and Aggregation of Uncharged Polyaromatic Molecules at the Oil-Water Interface: A Molecular Dynamics Simulation Study. *The Journal of Physical Chemistry B* **2014**, .

(25) Kuznicki, T.; Masliyah, J. H.; Bhattacharjee, S. Aggregation and Partitioning of Model Asphaltenes at Toluene− Water Interfaces: Molecular Dynamics Simulations. *Energy Fuels* **2009**, *23*, 5027-5035.

(26) Ruiz-Morales, Y.; Mullins, O. C. Coarse-Grained Molecular Simulations to Investigate Asphaltenes at the Oil–Water Interface. *Energy Fuels* **2015**, *29*, 1597-1609.

(27) Liu, J.; Zhao, Y.; Ren, S. Molecular Dynamics Simulation of Self-Aggregation of Asphaltenes at an Oil/Water Interface: Formation and Destruction of the Asphaltene Protective Film. *Energy Fuels* **2015**, *29*, 1233-1242.

(28) Mikami, Y.; Liang, Y.; Matsuoka, T.; Boek, E. S. Molecular Dynamics Simulations of Asphaltenes at the oil–water Interface: From Nanoaggregation to Thin-Film Formation. *Energy Fuels* **2013**, *27*, 1838-1845.

(29) Hu, C.; Garcia, N. C.; Xu, R.; Cao, T.; Yen, A. T.; Garner, S. A.; Macias, J. M.; Joshi, N.; Hartman, R. L. Interfacial Properties of Asphaltenes at the Heptol-Brine Interface. *Energy Fuels* **2015**, .

(30) Fan, Y.; Simon, S.; Sjöblom, J. Interfacial Shear Rheology of Asphaltenes at oil–water Interface and its Relation to Emulsion Stability: Influence of Concentration, Solvent Aromaticity and Nonionic Surfactant. *Colloids Surf. Physicochem. Eng. Aspects* **2010**, *366*, 120-128.

(31) López-Linares, F.; Carbognani, L.; González, M. F.; Sosa-Stull, C.; Figueras, M.; Pereira-Almao, P. Quinolin-65 and Violanthrone-79 as Model Molecules for the Kinetics of the Adsorption of C7 Athabasca Asphaltene on Macroporous Solid Surfaces. *Energy Fuels* **2006**, *20*, 2748-2750.

(32) González, M. F.; Stull, C. S.; López-Linares, F.; Pereira-Almao, P. Comparing Asphaltene Adsorption with Model Heavy Molecules Over Macroporous Solid Surfaces. *Energy Fuels* **2007**, *21*, 234-241.

(33) Schuler, B.; Meyer, G.; Peña, D.; Mullins, O. C.; Gross, L. Unraveling the Molecular Structures of Asphaltenes by Atomic Force Microscopy. *J. Am. Chem. Soc.* **2015**, *137*, 9870-9876.

(34) Sato, T.; Araki, S.; Morimoto, M.; Tanaka, R.; Yamamoto, H. Comparison of Hansen Solubility Parameter of Asphaltenes Extracted from Bitumen Produced in Different Geographical Regions. *Energy Fuels* **2014**, *28*, 891-897.

(35) Yang, F.; Tchoukov, P.; Dettman, H.; Teklebrhan, R. B.; Liu, L.; Dabros, T.; Czarnecki, J.; Masliyah, J.; Xu, Z. Asphaltene Subfractions Responsible for Stabilizing Water-in-Crude Oil Emulsions. Part 2: Molecular Representations and Molecular Dynamics Simulations. *Energy Fuels* **2015**, *29*, 4783-4794.

(36) Neeson, M. J.; Chan, D. Y.; Tabor, R. F. Compound Pendant Drop Tensiometry for Interfacial Tension Measurement at Zero Bond Number. *Langmuir* **2014**, *30*, 15388-15391.

(37) Schüttelkopf, A. W.; Van Aalten, D. M. F. PRODRG: A Tool for High-Throughput Crystallography of Protein-Ligand Complexes. *Acta Crystallographica Section D: Biological Crystallography* **2004**, *60*, 1355-1363.

(38) Oostenbrink, C.; Villa, A.; Mark, A. E.; Van Gunsteren, W. F. A Biomolecular Force Field Based on the Free Enthalpy of Hydration and Solvation: The GROMOS Force-Field Parameter Sets 53A5 and 53A6. *Journal of Computational Chemistry* **2004**, *25*, 1656-1676.

(39) Berendsen, H. J. C.; Postma, J. P. M.; van Gunsteren, W.; Hermans, J. In *Interaction Models for Water in Relation to Protein Hydration.* Pullmann, B., Ed., Ed.; In Intermolecular Forces; D. Reidel Publishing Company: Dordrecht, 1981.; pp 331-342.

(40) Hess, B.; Kutzner, C.; Van Der Spoel, D.; Lindahl, E. GRGMACS 4: Algorithms for Highly Efficient, Load-Balanced, and Scalable Molecular Simulation. *Journal of Chemical Theory and Computation* **2008**, *4*, 435-447.

(41) Van Der Spoel, D.; Lindahl, E.; Hess, B.; Groenhof, G.; Mark, A. E.; Berendsen, H. J. C. GROMACS: Fast, Flexible, and Free. *Journal of Computational Chemistry* **2005**, *26*, 1701-1718.

(42) Lindahl, E.; Hess, B.; van der Spoel, D. GROMACS 3.0: A Package for Molecular Simulation and Trajectory Analysis. *Journal of Molecular Modeling* **2001**, *7*, 306-317.

(43) Berendsen, H. J. C.; van der Spoel, D.; van Drunen, R. GROMACS: A Message-Passing Parallel Molecular Dynamics Implementation. *Comput. Phys. Commun.* **1995**, *91*, 43-56.

(44) Broemstrup, T.; Reuter, N. Molecular Dynamics Simulations of Mixed acidic/zwitterionic Phospholipid Bilayers. *Biophys. J.* **2010**, *99*, 825-833.

(45) Zhang, Y.; Feller, S. E.; Brooks, B. R.; Pastor, R. W. Computer Simulation of liquid/liquid Interfaces. I. Theory and Application to octane/water. *J. Chem. Phys.* **1995**, *103*, 10252-10266.

(46) Parrinello, M.; Rahman, A. Polymorphic Transitions in Single Crystals: A New Molecular Dynamics Method. *J. Appl. Phys.* **1981**, *52*, 7182-7190.

(47) Bussi, G.; Donadio, D.; Parrinello, M. Canonical Sampling through Velocity-Rescaling. *arXiv preprint arXiv:0803.4060* **2008**, .

(48) Essmann, U.; Perera, L.; Berkowitz, M. L.; Darden, T.; Lee, H.; Pedersen, L. G. A Smooth Particle Mesh Ewald Method. *J. Chem. Phys.* **1995**, *103*, 8577.

(49) Miyamoto, S.; Kollman, P. A. Settle: An Analytical Version of the SHAKE and RATTLE Algorithm for Rigid Water Models. *J. Comput. Chem.* **1992**, *13*, 952-962.

(50) Hess, B. P-LINCS: A Parallel Linear Constraint Solver for Molecular Simulation. *Journal of Chemical Theory and Computation* **2008**, *4*, 116-122.

(51) van Buuren, A. R.; Marrink, S. J.; Berendsen, H. J. A Molecular Dynamics Study of the decane/water Interface. *J. Phys. Chem.* **1993**, *97*, 9206-9212.

(52) Kunieda, M.; Nakaoka, K.; Liang, Y.; Miranda, C. R.; Ueda, A.; Takahashi, S.; Okabe, H.; Matsuoka, T. Self-Accumulation of Aromatics at the Oil− Water Interface through Weak Hydrogen Bonding. *J. Am. Chem. Soc.* **2010**, *132*, 18281-18286.

(53) Humphrey, W.; Dalke, A.; Schulten, K. VMD: Visual Molecular Dynamics. *J. Mol. Graph.* **1996**, *14*, 33-38.

(54) Saien, J.; Akbari, S. Interfacial Tension of Toluene Water Sodium Dodecyl Sulfate from (20 to 50) C and pH between 4 and 9. *Journal of Chemical & Engineering Data* **2006**, *51*, 1832-1835.

(55) Nordgård, E. L.; Landsem, E.; Sjöblom, J. Langmuir Films of Asphaltene Model Compounds and their Fluorescent Properties. *Langmuir* **2008**, *24*, 8742-8751.

(56) Andrews, A. B.; McClelland, A.; Korkeila, O.; Demidov, A.; Krummel, A.; Mullins, O. C.; Chen, Z. Molecular Orientation of Asphaltenes and PAH Model Compounds in Langmuir− Blodgett Films using Sum Frequency Generation Spectroscopy. *Langmuir* **2011**, *27*, 6049-6058.

(57) Rane, J. P.; Pauchard, V.; Couzis, A.; Banerjee, S. Interfacial Rheology of Asphaltenes at oil–water Interfaces and Interpretation of the Equation of State. *Langmuir* **2013**, *29*, 4750-4759.

(58) Yeung, A.; Dabros, T.; Masliyah, J. Does Equilibrium Interfacial Tension Depend on Method of Measurement? *J. Colloid Interface Sci.* **1998**, *208*, 241-247.

(59) Rosen, M. J.; Kunjappu, J. T. In *Surfactants and interfacial phenomena;* John Wiley & Sons: 2012; .

(60) Hu, Y.; Lv, W.; Zhao, S.; Shang, Y.; Wang, H.; Liu, H. Effect of Surfactant SDS on DMSO Transport Across water/hexane Interface by Molecular Dynamics Simulation. *Chemical Engineering Science* **2015**, *134*, 813-822.

(61) Pradines, V.; Krägel, J.; Fainerman, V. B.; Miller, R. Interfacial Properties of Mixed β-Lactoglobulin− SDS Layers at the water/air and water/oil Interface. *The Journal of Physical Chemistry B* **2008**, *113*, 745-751.

(62) Rane, J. P.; Harbottle, D.; Pauchard, V.; Couzis, A.; Banerjee, S. Adsorption Kinetics of Asphaltenes at the oil–water Interface and Nanoaggregation in the Bulk. *Langmuir* **2012**, *28*, 9986-9995.

(63) Pauchard, V.; Rane, J. P.; Banerjee, S. Asphaltene-Laden Interfaces Form Soft Glassy Layers in Contraction Experiments: A Mechanism for Coalescence Blocking. *Langmuir* **2014**, *30*, 12795-12803.

TOC:

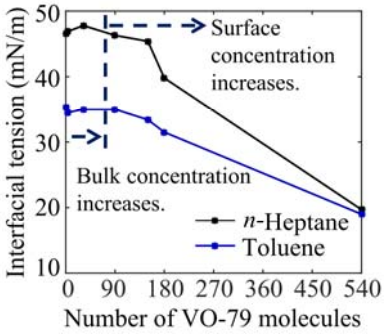
Interfacial tension (mN/m)
50
40
30
20
10
0
90
180
270
360
450
540
Number of VO-79 molecules
Surface concentration increases.
Bulk concentration increases.
n-Heptane
Toluene